Integrated Hull Design, Boundary-Layer Control, and Propulsion of Submerged Bodies

F. R. GOLDSCHMIED*
University of Utah, Salt Lake City, Utah

Power requirements of large submerged bodies at high Reynolds numbers are optimized by the hydrodynamic synthesis of body design, boundary-layer control, and propulsion. Conventional rigid skin, all turbulent boundary layers, and a single suction slot are accepted as realistic engineering constraints. A 3:1 body has been designed and has been tested in a wind tunnel at a Reynolds number of 10^7; the wake drag has been found to be $C_{Dw} = 0.002$, and the equivalent suction drag $C_{Ds} = 0.0142$ yielding a total equivalent drag $C_D = 0.0162$ (based on volume). This can be compared to $C_D = 0.0235$ for the best conventional streamlined body (Akron airship model). A total engine power coefficient has also been determined, $C_P{}^* = 0.01585$, while a conventional streamlined vehicle with stern wake propeller has a $C_P{}^* = 0.0215$, thereby showing a net gain of 26%. There is a possible tradeoff between suction and propulsion powers allowing the total power coefficient to decrease to $C_P{}^* = 0.0100$ and to reach a 50% power gain.

Nomenclature

x = axial distance
y = radial distance
c = airfoil chord
L = body length
X = x/c or x/L, dimensionless axial length
Y = y/c or y/L, dimensionless radial length
g = suction slot width
δ = boundary-layer thickness
δ^* = boundary-layer displacement thickness
θ = boundary-layer momentum thickness
d = body diameter
V = useful enclosed body volume
D_s = equivalent suction drag
D_w = wake drag
T = thrust
W_s = power charged to boundary-layer-control suction
W_w = power charged to propulsion (counteracting the wake drag)
U = fluid velocity outside the boundary layer
u = fluid velocity within boundary layer
U_{s_1} = velocity entering propulsor, relative to body
U_{s_2} = velocity leaving propulsor, relative to body
ρ = fluid mass density
μ = fluid absolute viscosity
ν = fluid kinematic viscosity
R_L = U_0L/ν, body Reynolds number
R_θ = $U_1\theta_1/\nu$, momentum-thickness Reynolds number upstream of discontinuity
m_s = total suction mass flow rate
C_m = $m_s/\rho U_0L^2$, total suction mass flow coefficient
Q = $m_s/\rho\pi d_1$, suction volume flow per unit slot length
C_Q = $Q/U_1\theta_1$, suction flow coefficient
C_H = $2\Delta H_1/\rho U_1{}^2$, suction head coefficient
q = $\frac{1}{2}\rho U_0{}^2V^{2/3}$, denominator of drag coefficient
C_{Ds} = D_s/q, equivalent suction-drag coefficient
C_{Dw} = D_w/q, wake-drag coefficient
C_D = D/q, total drag coefficient
C_T = T/q, thrust coefficient
C_{Ps} = W_s/qU_0, suction-power coefficient
C_{Pw} = W_w/qU_0, propulsion-power coefficient
C_P = total power coefficient
η_P = shrouded impeller's pump efficiency
η_T = propulsive efficiency
$C_P{}^*$ = C_p/η_P, total engine power coefficient
BLC = boundary-layer control

Subscripts

0 = freestream condition
1 = upstream of discontinuity
2 = downstream of discontinuity
3 = body trailing edge
x = lengthwise position on body or airfoil
s = pertaining to boundary-layer-control suction
w = pertaining to the wake

Presented as Paper 66-658 at the AIAA Second Propulsion Joint Specialist Conference, Colorado Springs, Colo., June 13–17, 1966; submitted June 13, 1966; revision received January 3, 1967. This work was funded by the U. S. Navy, Office of Naval Research, under Contract NOnr 1412(00) L1. [3.09, 4.22]

* Associate Research Professor, Mechanical Engineering Department and Director, Fluid Control Systems Laboratory. Member AIAA.

1. Introduction

AN investigation of an engine/airframe, propulsion/boundary-layer-control/body design synthesis was proposed in 1954 by Goldschmied[1] to the Office of Naval Research (ONR) for airship application (Reynolds number over 10^8). It was believed from preliminary estimates that there was a good chance to achieve substantial gains in power requirements, within realistic engineering constraints of naval airships.

Another power-reduction method was also considered at that time for airships, i.e., the stern propeller as applied to a conventional streamlined hull to extract energy from the wake. This was investigated in a large wind tunnel much later (1962) by McLemore[2] and found to offer worthwhile power gains (as compared to car-mounted or fin-mounted propellers).

The inviscid body design and the boundary-layer-control analysis were performed in 1954 with ONR funding. This work is reported in Ref. 3. Later a wind-tunnel model was designed, and in 1956 a series of wind-tunnel tests was performed at the David Taylor Model Basin, at Reynolds numbers up to 1.2×10^7, comparing the new design directly with a conventional airship model hull. The experimental results have been reported by Cerreta[4] in 1957. No further test work was carried out because of the vanishing interest in naval airship development. A final summary report of the investigation up to 1957 is given by Ref. 5. It is unfortunate that, despite the excellent results of the first wind-tunnel tests, a self-propelled model was not built and tested in a large wind tunnel, such as used by McLemore.[2]

A review of the wind-tunnel results and a new propulsion analysis were undertaken by the author in 1965–1966 as personal research at the University of Utah. It is the au-

thor's belief, however, that this aerodynamic research work transcends mere airship application and has basic import to submerged self-propelled bodies in general. This belief is the motivation for the present paper, after due consideration of the hydrodynamic progress made in the last ten years and the present state-of-the-art in underwater propulsion and drag reduction at high Reynolds numbers.

2. Hydrodynamic Approach

The present approach to the power optimization of self-propelled submerged bodies at high Reynolds numbers (over 10^9) is based on a hydrodynamic synthesis of hull design, boundary-layer control, and propulsion, considering the following well-known and accepted factors.

2.1 Reference Criteria

It is important to set forth the reference quantities to be used in the definition of classification criteria. Here the useful enclosed volume V and the engine's power expenditure (hp) will be used for reference in the definition of a power coefficient

$$C_P{}^* = \frac{\text{hp}}{V^{2/3}\frac{1}{2}\rho U_0{}^3} \tag{1}$$

"Drag" coefficients are semantically detrimental in the present investigation, although traditional in many hydrodynamic fields. Control and exploitation of the boundary-layer kinetic energy are the cornerstones of the present synthesis.

2.2 Reynolds Number Effects

Large Reynolds numbers up to and over 10^9 are considered in this investigation. The consequences are that the extent of the reliable laminar boundary layer on the body will be negligible (over $R_x = 10^7$) despite favorable pressure gradients, and even despite boundary-layer control by distributed area suction or damping skins. Also the possibility of severe hull vibrations militates against the chances of laminar flow, without mentioning the usual skin protuberances, irregularities, and barnacles. Thus as a practical matter, turbulent boundary layers must be accepted throughout.

2.3 Boundary-Layer Control

Turbulent boundary-layer control on a conventional streamlined body is concerned with the prevention of flow separation on the aftbody. This job is complicated by the high sensitivity of the flow to body angle of attack, creating three-dimensional separation contours, and also by the dependence of the separation point on the Reynolds number. Thus, a single suction slot which proves adequate in a wind-tunnel test at zero angle can offer no assurances for a prototype in actual operation. In general, when the adverse pressure-gradient area extends over 60–75% of the body length, a fixed slot will encounter a very wide variation of boundary-layer thicknesses and profiles. A stern pump-jet (on conventional body) is a single suction slot well aft (for *BLC* purposes), subject to all the difficulties and limitations of the single slot. On the other hand, distributed area suction may be used over the aforementioned 60–75% length to control the boundary-layer growth in its entirety. However, this is not deemed quite practical because the porous skin is structurally weak (prone to failure, especially in fatigue) and easy to clog, particularly in seawater. Furthermore, the ducting needed over the body under the large suction area will take up some useful volume and thereby increase the C_P value. A multiple-ring-slot skin has also been used, obviating the problems of fatigue and clogging. However, the suction quantities required are larger and are a function of the number of slots.

Then the fluid which has been sucked into the body must be pumped up to freestream static pressure and to flight velocity so that it may leave the body ideally at "zero" velocity relative to body ($U_{s_1} = U_{s_2} = 0$). This usually takes much power and it is never worthwhile unless it buys a substantial reduction in propulsion power per unit body volume.

It has been observed, however, that once this boundary-layer-control fluid has been brought up to zero relative velocity, it will enable a reaction propulsor to produce thrust in the most economical manner. Thus, only in the combination with propulsion has boundary-layer control proved advantageous powerwise.

2.4 Trailing-Edge Full Suction

It is well-known that it is more efficient powerwise to suck all the turbulent boundary layer on a flat plate at its trailing edge and to complete mechanically its energization to flight velocity than to allow it to pour its kinetic energy into a natural wake requiring thrust to counteract the drag force. In the former case, the pump power required to complete the boundary-layer energization is given by:

$$\frac{W_s}{\frac{1}{2}\rho U_0{}^3} = \eta_P \int_0^\infty \frac{u}{U_0}\left[1 - \frac{u}{U_0}\right]^2 dy \tag{2}$$

In the latter case, the thrust power required to overcome to wake drag is given by

$$\frac{W_w}{\rho U_0{}^3} = \eta_T \int_0^\infty \frac{u}{U_0}\left[1 - \frac{u}{U_0}\right] dy \tag{3}$$

If the pump efficiency η_P is equal to the propulsive efficiency η_T, the theoretical gain for a turbulent boundary layer is of the order of 10%.

2.5 Boundary-Layer-Intake Propulsion

It is well-known and accepted that it is much more efficient powerwise to use boundary-layer fluid (rather than freestream fluid) to feed the propulsor because this fluid possesses energy gained from the body. Thrust gains can be made, with apparent propulsive efficiencies increased (based on freestream velocity) up to 140%.[2] So-called wake propellers, designed to match the stern boundary-layer profile of a particular body at a particular Reynolds number, have been used successfully to regenerate wake energy and so have some pump-jets with boundary-layer intake. However, there are two problems here; first, a hull drag increment is created by these stern propulsors, in the nature of a hull pressure drag, this increment being given as 7–10%,[6] 12%,[7] and 19%[2]; then such propulsors are quite sensitive to angle of attack.

2.6 Fineness-Ratio Effect

The optimum fineness ratio of streamlined bodies (on the basis of enclosed volume) has been found experimentally to be between 5:1 and 6:1. Here the sum of skin friction and pressure drag is the lowest in relation to volume. These results have been determined in wind tunnels and water channels at Reynolds numbers in the vicinity of 10^7. As the Reynolds number increases, the skin friction will decrease but the pressure drag will increase according to the turbulent separation criterion of Goldschmied.[8] This means that the optimum fineness ratio will increase. If the pressure drag could be controlled or eliminated by boundary-layer control, the optimum fineness ratio will decrease toward unity, for minimum surface-area/body-volume ratio and consequent minimum skin friction and hull weight. At operational Reynolds numbers of 10^8 to 10^9, the boundary layer will always be turbulent even on the sphere.

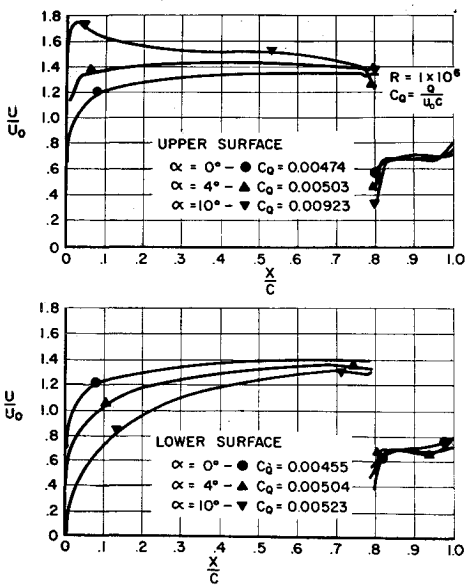

Fig. 1 Griffith 30% airfoil with suction boundary-layer control. Note that 30% Griffith airfoil is very similar to 34% Lighthill airfoil. (See Ref. 14).

2.7 Griffith Airfoil Concept

The stepwise velocity distribution concept of Griffith, as embodied by Lighthill's[9] direct-design-at-incidence inviscid method, yields airfoils with favorable pressure gradients throughout, up to a specified angle of attack, except for a pressure discontinuity. This discontinuity is actually a very steep pressure gradient over a small-enough width so that a single suction slot is able to encompass the area and to allow the boundary layer to cross the discontinuity. The location of the discontinuity does not change with angle of attack and also its pressure ratio remains substantially the same. It has been shown experimentally on airfoils up to 34% thick that the Griffith concept is valid over a range of angles of attack and that the pressure drag is reduced to negligible values for any thickness, as long as the boundary-layer suction is adequate at the discontinuity.

3. Axisymmetric Hull Design

In 1943 Richards and Burge[10] reported the results of small-scale wind-tunnel tests of a new type of airfoil. This scheme arose from a suggestion by A. A. Griffith and consisted in designing the airfoil so that in inviscid (potential) flow it had a stabilizing favorable velocity gradient along the whole chord, except at one position (well aft) where a velocity discontinuity occurred. Thus if sufficient suction was applied at this one point to prevent separation of the boundary layer crossing the sudden pressure rise (similar to a shock wave), laminar boundary-layers might be expected throughout (if the Reynolds number was not too high and the surface was smooth and clean enough), regardless of airfoil thickness and of the angle of attack (up to some desired value).

The first airfoil was designed by the method of Goldstein with a 16% thickness. A great deal of aerodynamic development was carried out subsequently both in England and in Australia with airfoils up to 34% thickness. This effort culminated in full-scale glider tests in Australia from 1948 to 1951. A brief history of the Griffith airfoil development is given by Head[11] and by Thwaites.[12] The airfoil is also mentioned by Schlichting[13] in his well-known book (pp. 283, 284).

Figure 1 shows the velocity distribution on a 30% symmetrical Griffith airfoil, as determined in the wind tunnel by Gregory and Walker[14] for three angles of attack 0°, 4°, and 10°. At $\alpha = 0°$ the velocity-ratio peaks at 1.4 and at $\alpha = 10°$ it peaks at only 1.7. The discontinuity is at $x/c = 0.80$ for all α values and the upstream velocity ratio is 1.4 regardless of α. The suction flow needed is increased only 55% from $\alpha = 0°$ to $\alpha = 10°$ (as indicated by the C_Q coefficient). Thus, it is seen that this airfoil will operate in the desired manner in an α angle range $\pm 10°$.

For ease of comparison, a conventional low-drag 12% NACA airfoil velocity distribution is depicted in Fig. 2 for the same values of α. At $\alpha = 0°$ the velocity ratio peaks at 1.2 (lower than 1.4) at $x/c = 0.35$, but at $\alpha = 10°$ it peaks at 2.8 (much higher than 1.7) at $x/c = 0.01$. It is the performance at $\alpha = 10°$ that really tells the difference between the two airfoils! Of course, the reasons behind the application of the Griffith concept to bodies are quite different from those which motivated the extensive airfoil development. These reasons will become more apparent later in the present paper.

The first problem in the axisymmetric hull design according to the Griffith concept is the lack of a body method comparable to that of Lighthill[9] for direct design at incidence of inviscid airfoils. Analytical methods for the calculation of incompressible inviscid velocity distribution over axisymmetric bodies have been investigated and applied by Goldschmied.[15] They are of little use for the present design problem. A thorough discussion of uniform flow past bodies of revolution is given by Thwaites[16] in his book on incompressible aerodynamics.

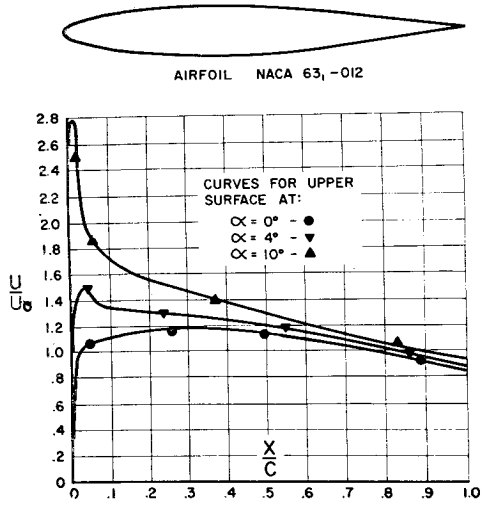

Fig. 2 Typical conventional low-drag NACA airfoil.

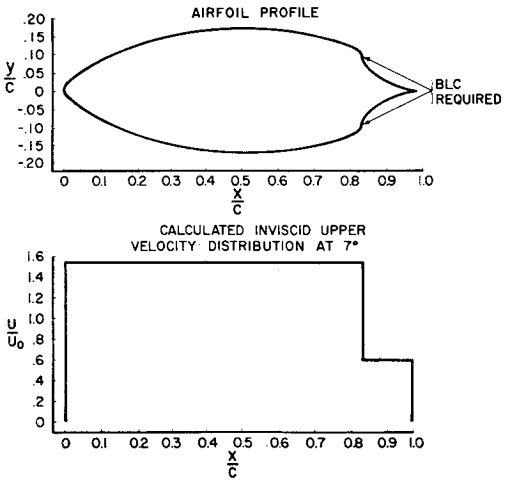

Fig. 3 Lighthill 34% airfoil designed directly for 7° angle of attack.

It was decided to achieve first a two-dimensional airfoil shape by Lighthill's method. Appendix IV of Ref. 9 already presents the complete calculations for a 34% symmetrical airfoil with the discontinuity at 83%, designed for constant velocity over the forebody and over the aftbody at $\alpha = 7°$. The airfoil profile and the velocity distribution for $\alpha = 7°$ are shown in Fig. 3. Furthermore Appendix V of Ref. 9 presents the complete calculations for a 48% symmetrical airfoil with the discontinuity at 89%, designed for constant velocity over the forebody and over the aftbody at $\alpha = 12°$. These airfoil profiles have been calculated for two-dimensional inviscid flow. The expected boundary-layer displacement thickness δ^* should be subtracted from the calculated profile.

It was decided to use the 34% profile to yield a 3:1 body with adequate angle-of-attack range. The next problem was to convert the two-dimensional profile into the corresponding axisymmetric shape. For this purpose the analog electric tank lends itself beautifully because the same tank can either be used horizontally (two-dimensional analog) or slanted at 10° (axisymmetric analog) as shown by Cheers and Rayner,[17] Goldschmied,[18] etc. Figure 4 shows the inviscid velocity distribution obtained in the electric tank for both cases at zero angle of attack.

Table 1 Step velocity profiles

Airfoil profile table		Body profile table	
X	Y	X	Y
0.000000	0.000000	0.0000	0.00000
0.002063	0.007785	0.0326	0.06462
0.006973	0.016421	0.1007	0.08215
0.014770	0.025675	0.1348	0.0966
0.024319	0.035314	0.1691	0.1094
0.037017	0.045195	0.2029	0.1204
0.051396	0.055201	0.2368	0.1302
0.067808	0.065227	0.2710	0.1384
0.086151	0.075182	0.3021	0.1451
0.106321	0.084979	0.3391	0.1515
0.128209	0.094540	0.3735	0.1573
0.151701	0.103791	0.4073	0.1617
0.203011	0.121087	0.4409	0.1652
0.23052	0.129013	0.4751	0.1678
0.259223	0.136370	0.5093	0.1694
0.288824	0.143124	0.5431	0.1698
0.350300	0.154588	0.5771	0.1688
0.381861	0.159221	0.6110	0.1666
0.413769	0.163073	0.6454	0.1633
0.445866	0.166109	0.6792	0.1585
0.509968	0.169658	0.7128	0.1521
0.541652	0.170011	0.7261	0.1490
0.572896	0.169345	0.7346	0.1469
0.603514	0.167752	0.7431	0.1446
0.662218	0.161698	0.7516	0.1412
0.689991	0.157332	0.7600	0.1395
0.716497	0.152094	0.7684	0.1367
0.741531	0.145816	0.7770	0.1335
0.764888	0.138449	0.7855	0.1302
0.786312	0.129888	0.7941	0.1265
0.805419	0.119934	0.8026	0.1224
0.821777	0.107971	0.8109	0.1176
0.830155	0.097124	0.8198	0.1113
0.8300542	0.093303	Discontinuity point	
0.831546	0.083391	0.8283	0.09795
0.836909	0.073538	0.8446	0.07690
Discontinuity point		0.8615	0.06132
0.850899	0.058587	0.8786	0.04872
0.880142	0.036137	0.8956	0.03778
0.909930	0.021419	0.9126	0.02709
0.936557	0.011761	0.9295	0.01746
0.959021	0.005717	0.9462	0.00889
0.976821	0.002250	0.9635	0.00318
0.989670	0.000552	0.9806	0.00047
1.000000	0.000000	1.0000	0.00000

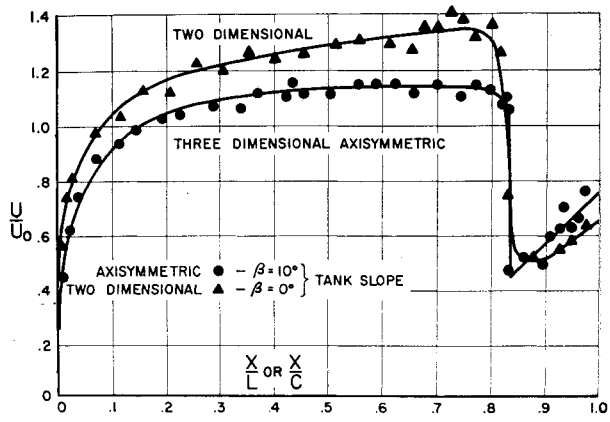

Fig. 4 Inviscid velocity distribution as obtained in electric analog tank.

Thus, the determination of the inviscid body shape is partly analytical by Lighthill's method and partly experimental in the electric analog tank. It is to be noted that the stern now ends into a sharp trailing point, with no allowance for a finite stern-propulsion jet. Necessary design modifications are to be considered later in the final integrated design. Similarly, the inviscid body design gives no information on the detailed suction-slot arrangement. For convenient reference, both the 34% airfoil profile (from Ref. 9, Appendix IV) and the final body profile[4] are tabulated in Table 1. A schematic is provided in Fig. 5 showing nomenclature and coordinates.

It is to be noted that the aftbody, past the discontinuity, has not been included in the useful volume, because it will be occupied mainly by the impeller and associated ducting.

Typical wind-tunnel test results from Ref. 4 are shown in Fig. 6, where the experimental points (at Reynolds number of 1.1×10^7 and at the best suction-slot width) are superimposed on the inviscid velocity distribution (as determined in the electric analog tank). The agreement is seen to be excellent, except for the slight sink effect just upstream of the discontinuity. This discrepancy could be corrected by a very slight recontouring of the body. The velocity ratio across the discontinuity is 1.2/0.6 = 2.0. This yields a large pressure recovery over a negligible axial span $g/L = 0.008$ or 0.8% of the body length, in full conformance with the Griffith concept of aerodynamic design. Furthermore, the velocity gradient is favorable both on the forebody and on the aftbody, giving "natural" control of the turbulent boundary layer in those areas.

It is unfortunate that the wind-tunnel tests were not extended to angles of attack other than zero. It is just the

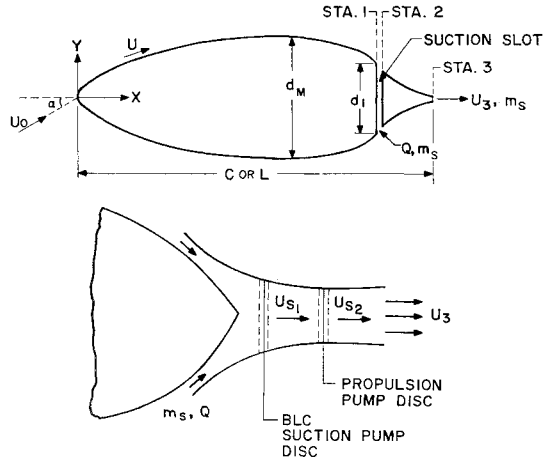

Fig. 5 Configuration sketch, including suction and propulsion.

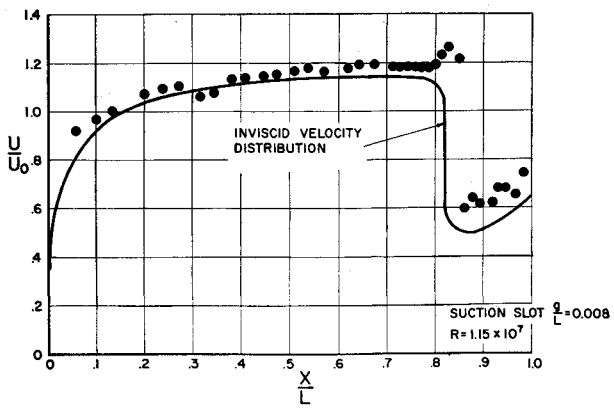

Fig. 6 Wind-tunnel velocity distribution with boundary-layer-control suction on axisymmetric hull. Data from Ref. 4.

ability to handle a range of α angles that is one of the major claims for the present body design with boundary-layer control. In fact, flow about conventional streamlined bodies is quite sensitive to angle of attack. This is illustrated quite dramatically by Fig. 7 which portrays the contours of minimum pressure and of turbulent separation at $\alpha = 0°$, 6°, 12°, and 18° as determined experimentally in the wind tunnel by Freeman[19] and analytically by Allen[20] on an airship model. Recently this complex flow phenomenon has been studied both theoretically and experimentally by Rodgers.[21] It can be readily appreciated that these effects are quite significant for both drag and stern propulsion, i.e., for the manner in which energy is put by the body into the boundary layer and for the manner in which it can be regenerated to useful purposes.

4. Boundary-Layer Analysis

The boundary-layer analysis comprises the forebody boundary-layer calculation and the analysis of boundary-layer control at the discontinuity in regard to suction flow, pressure, and power, and in regard to boundary-layer growth as a function of suction. The aftbody boundary-layer calculation and the wake-drag computation are then carried out to complete the boundary-layer analysis. It is assumed that there is no pressure drag at all.

The understanding of Reynolds number effects is believed to be adequate to provide exact extrapolation to larger bodies at higher velocities because there are no problems of turbulent boundary-layer growth under adverse pressure gradients and of turbulent separation in three dimensions (see Fig. 7), up to $\alpha = 7°$.

4.1 Forebody Boundary Layer

The computation of the axisymmetric boundary layer under favorable velocity gradients on the forebody does not present any difficulty either for the laminar or the turbulent case. The location of laminar/turbulent transition cannot be predicted exactly, but this is seldom important for large bodies, because at high Reynolds numbers the laminar region is of negligible extent anyway. (1–10% length). F. W. Boltz[22] has explored experimentally the problem of transition on bodies, flat plates, and wings. In the wind-tunnel tests of Ref. 4, since the body Reynolds number was only 10^7, transition was carefully triggered for all tests at 10% length by a double row of staggered, discrete, conical turbulence-stimulating elements. A sublimation technique was used to check on the actual occurrence of transition. In this manner, the experimental boundary-layer data can be interpreted exactly.

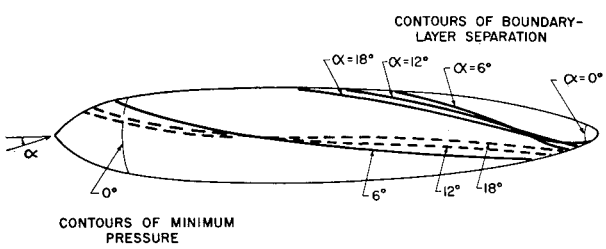

Fig. 7 Contours of minimum pressure and of flow separation on "Akron" hull at angles of attack. (See Refs. 19 and 20.)

The quadrature method of Truckenbrodt[23] has been selected for the computation of the momentum thickness θ_1, upstream of the discontinuity. All the suction coefficients at the discontinuity use θ_1 as the reference length

$$\frac{\theta_1}{L} = \frac{\left[C_1^* + \left(\frac{C_f}{2}\right)^{1+n} \int_{x/L}^{x_1/L} \left(\frac{U}{U_0}\right)^{3+2n} \left(\frac{y}{L}\right)^{1+n} d\left(\frac{x}{L}\right)\right]^{1/1+n}}{\left(\frac{U_0}{U}\right)^3 \left(\frac{y}{L}\right)} \tag{4}$$

$$C_1^* = \left[\frac{U_x}{U_0} \cdot \frac{y_x}{L} \cdot \frac{\theta_x}{L}\right]^{1+n} \quad \text{integration constant} \tag{5}$$

$$C_1^* = \left\{\frac{C_f}{2}\left[\int_0^{x/L} \left(\frac{U}{U_0}\right)^5 \left(\frac{Y}{L}\right)^2 d\left(\frac{x}{L}\right)\right]^{1/2}\right\}^{1+n} \tag{6}$$

$$C_{ft} = \frac{0.036}{(U_0 L/\nu)^{1/7}} \quad \text{turbulent friction} \tag{7}$$

$$C_{fl} = \frac{1.328}{(U_0 L/\nu)^{1/2}} \quad \text{laminar friction} \tag{8}$$

If turbulent flow is assumed from the nose, as it is proper for the case of high Reynolds numbers, then $C_1^* = 0$. For the wind-tunnel tests where transition was fixed at 10% length, then C_1^* must be computed from Eq. (6) from $x = 0$ to $x = 0.10L$ using C_{fl} from Eq. (8). It is seen from Table 2 that H is between 1.43 and 1.52, indicating a good healthy boundary-layer profile upstream of the velocity discontinuity.

For the laminar case $n = 1.0$ and for the turbulent case $n = \frac{1}{6}$. In Fig. 8 there are represented the experimental momentum-thickness points (taken at 79.5% length), the same points corrected theoretically to 83%, and the theoretical θ_1 curves at both 79.5 and 83% length. It is seen that the wind-tunnel points are somewhat lower than the curves by about 15% at $R_L = 10^7$. For convenience, the data of Ref. 4 are reproduced in Table 2 for the case of minimum

Table 2 Boundary-layer wind-tunnel data

R_L	δ_1^*	θ_1	$H = \delta^*/\theta$
4.51×10^6	0.1047	0.0705	1.485
4.41	0.947	0.622	1.522
4.51	0.0888	0.0609	1.458
4.60	0.0827	0.0553	1.495
7.15	0.0948	0.0624	1.519
7.20	0.0833	0.0572	1.456
7.10	0.0802	0.0562	1.427
7.10	0.0878	0.0584	1.503
10.15	0.0848	0.0563	1.506
10.0	0.0793	0.0553	1.434
4.36	0.0833	0.0582	1.431
6.95	0.0880	0.0608	1.447
7.10	0.0846	0.0581	1.456
7.05	0.0799	0.0558	1.432
6.95	0.0819	0.0562	1.457
9.8	0.0795	0.0550	1.445
10.2	0.0777	0.0537	1.447
10.1	0.0791	0.0552	1.433
11.3	0.0786	0.0547	1.437

suction with a slot width $g/L = 0.008$ (boundary-layer rake at $s/L = 0.795$ and note that $L = 58.80$ in.).

4.2 Boundary-Layer Control at the Velocity Discontinuity

In the body design the location of the velocity discontinuity has been placed at 83% length. Here the velocity ratio changes abruptly from 1.2 to 0.6 and suction is required to allow the boundary layer to cross the 2:1 velocity step without separation. The best suction-slot width has been found in the wind tunnel to be $g/L = 0.008$ or $g/\theta_1 = 6$. Since the ratio of body-radius/momentum-thickness is large at the slot, $y_1/\theta_1 = 75$, the flow may be considered two-dimensional for the purposes of analysis. Thus, a large body of airfoil theory and experimental knowledge may be exploited for this present application.

G. I. Taylor suggested a simple argument to explain the behavior of the boundary-layer in crossing the velocity discontinuity. The argument has two basic assumptions: 1) There is no change in total head of a streamtube as it crosses the discontinuity. 2) The static pressure is constant through the boundary layer. The assumptions have been carefully examined experimentally by Gregory[24] and it is found that the suction-rate estimates are reasonable but that close agreement with actual velocity profiles is not obtained. In fact the change in head in a boundary-layer streamline as it crosses the discontinuity is small compared with changes in head normal to the streamline. However, static pressure changes through the boundary layer are observed to be large.

Preston, Gregory, and Rawcliffe[25] describe a method for assessing the performance of thick suction-slot airfoils, including the suction pump power, on the basis of Taylor's simple criterion. An equivalent total drag is formulated, comprising the actual wake drag and the suction drag (from the pump power). No attempt is made to include propulsion, since it is an airfoil section that is being studied. As it is well-known, suction fluid can be utilized, once aboard the vehicle, to increase the propulsive efficiency by substantial amounts.

The suction-flow coefficient C_Q is defined as follows, on the basis of the total suction mass flow m_s given in Ref. 4:

$$C_Q = \left(\frac{m_s}{\rho U_0 L^2}\right) \frac{1}{(\pi d_1/L)(\theta_1/L)(U_1/U_0)} = \frac{Q}{\theta_1 U_1} \qquad (9)$$

At $R_L = 10^7$, the approximate relation holds: $C_Q = 68.5\, m_s$. On the other hand

$$\frac{m_s}{\rho U_0 L^2} = C_Q \left(\frac{\pi d_1}{L}\right)\left(\frac{\theta_1}{L}\right)\left(\frac{U_1}{U_0}\right) = C_m \qquad (10)$$

Figure 9 displays the suction coefficient $C_Q = Q/U_1\theta_1$ against R_θ, where Q is taken according to the Taylor criterion per unit length of slot periphery. The wind-tunnel points

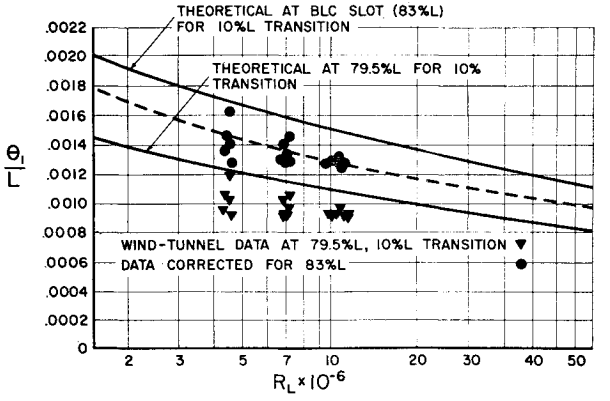

Fig. 8 Boundary-layer momentum thickness upstream of boundary-layer-control suction slot.

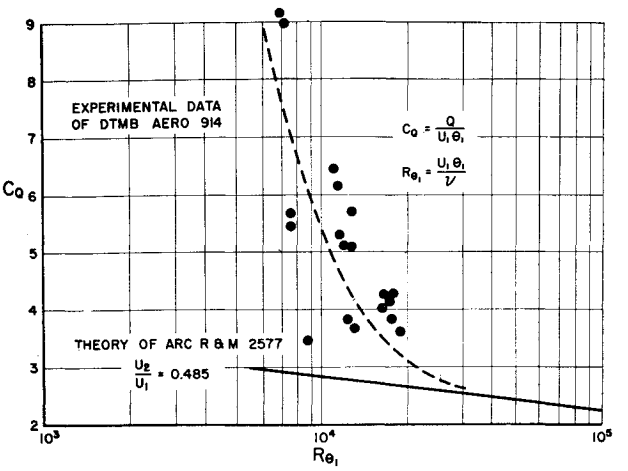

Fig. 9 Flow parameter for boundary-layer-control suction.

are also shown and are seen to have a very steep trend above the theoretical curve. The evidence is not adequate for firm conclusions but it does appear that at $R_\theta \gg 10^4$ there will be good agreement between theory and experiment.

Figure 10 presents the pressure coefficient $C_H = 2\Delta H_1/\rho U_1^2$ plotted against R_θ. It is seen that the points lie mainly below the theoretical line. Again it appears that there will be agreement for $R_\theta \gg 10^4$.

It is to be noted that the theoretical lines for C_Q and C_H are based on the minimum values for stabilization of the turbulent boundary layer crossing the discontinuity. Small changes in the body and slot contour may have substantial effects on the actual minimum C_Q and C_H. This would have to be shown by an organized wind-tunnel development program. It remains only to consider the boundary-layer momentum thickness θ_2 downstream of the discontinuity. Unfortunately θ_2 is not given directly in Ref. 4. It is calculated from the wake drag. The ratio θ_2/θ_1 is quite sensitive to the suction coefficient C_Q and to the upstream boundary-layer profile, as shown in Fig. 11. Two theoretical curves are plotted for $N = 5$ and $N = 7$, where N is the exponent of the turbulent boundary-layer power profile,

$$u/U_1 = (y/\delta)^{1/N} \qquad (11)$$

The N values were selected for best fit to the experimental points. At the experimental Reynolds number, C_Q should be less than 3 according to theory and, therefore, θ_2/θ_1 should be approximately 2.0. Actually, since the experimental C_Q were higher, θ_2/θ_1 ranged from 0.10 to 1.00.

The boundary-layer-control analysis is concluded with the knowledge of θ_1/L, C_Q, C_H, and θ_2/θ_1 for the given body velocity distribution. However, in practice C_Q, C_H, and θ_2/θ_1 depend more or less strongly on suction-slot design. The effect of suction-slot width and slot shape was investigated to some extent in the wind tunnel by Cerreta.[4] The drag coefficients at $R_L = 1.0 \times 10^7$ are shown in Table 3.

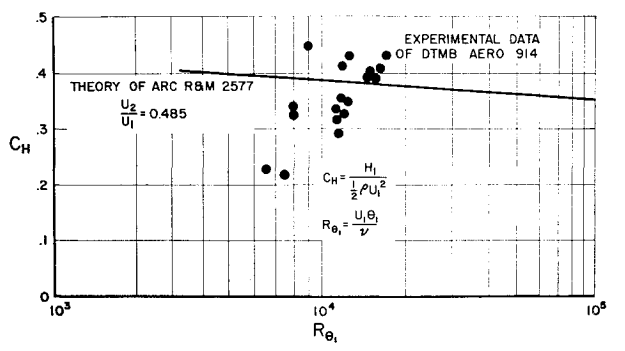

Fig. 10 Pressure parameter for boundary-layer-control suction.

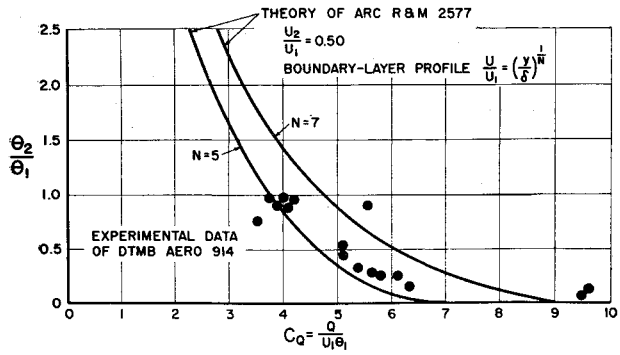

Fig. 11 Ratio of boundary-layer momentum thicknesses across boundary-layer control suction slot.

It is seen in Table 3 that the $g/L = 0.008$ slot gives the lowest suction power and the lowest total equivalent drag coefficient. In most cases the wake drag is small in comparison with the equivalent suction drag, in the ratios from 1:7 to 1:12. It is to be noted that the suction-flow coefficient C_Q is constant for all slot widths g/L, in the vicinity of 5.5.

4.3 Aftbody Boundary Layer and Wake Drag

The aftbody is entirely under a favorable pressure gradient, the velocity ratio rising from 0.6 to 0.8. Therefore, the computation of the momentum thickness θ_3 should not present any difficulty, once θ_2 has been established. Equations (4, 5, and 7) should be used. The boundary layer will always be turbulent, even at comparatively low Reynolds numbers. The form factor $H = \delta^*/\theta$ should remain in the range 1.4–1.5.

In the actual design of a complete self-propelled body, there will be a propulsion jet issuing from the stern, which will entrain the aftbody boundary layer as it leaves station 3 (see Fig. 5). This will act to reduce θ_3 and, therefore, the wake drag. Because of the lack of experimental information, this effect has not been included in the analysis.

Figure 12 shows the relationship between the wake-drag coefficient C_{Dw} and the momentum thickness θ_2/L downstream of the discontinuity. Since the wake drag has been measured in the wind-tunnel tests of Ref. 4, this curve has been employed to calculate θ_2 (which was not measured).

Figure 11 shows how θ_2 can be controlled by C_Q. This means that C_{Dw} can be controlled by C_Q and that the wake drag can be reduced by a factor of 10, for a suction increase

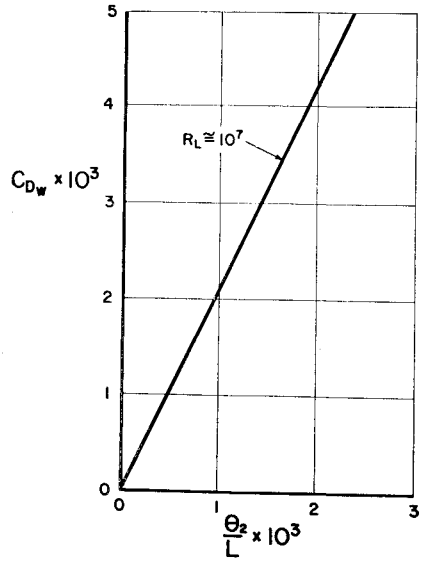

Fig. 12 Wake-drag coefficient vs boundary-layer momentum thickness after suction slot.

of the order of only 2! This possibility of tradeoff between suction power and thrust power opens new ways for the overall optimization of a self-propelled vehicle.

5. Power System Analysis

The successful integration of hull design, boundary-layer control, and propulsion requires a good understanding of the power-system analysis. The first concept to note is that the moving vehicle puts energy into the stationary fluid. The boundary layer is a reservoir of kinetic energy to be tapped and regenerated. The second concept is that power can be used to control this energy transfer between vehicle and fluid, given a suitable hull design. The third concept is that propulsion power is minimized when the boundary-layer-control suction pump brings a fluid mass flow m_s to zero relative velocity with the propulsor ($U_{s_1} = 0$). The reactive thrust is given by

$$T = m_s[U_{s_2} - U_{s_1}] = m_s U_0[(U_{s_2}/U_0) - (U_{s_1}/U_0)] \quad (12)$$

Assume that $T/m_s U_0 = 0.04$ (typical value for present design), with $U_{s_2}/U_0 = 1.04$ and $U_{s_1}/U_0 = 1.0$. The power required will be

$$W_w = \tfrac{1}{2} m_s U_0^2 [U_{s_2}^2/U_0^2 - U_{s_1}^2/U_0^2] \quad (13)$$

$$\frac{W_w}{\frac{1}{2} m_s U_0^2} = 0.08 \quad (14)$$

Assume now that while $T/m_s U_0 = 0.04$ still, the velocities are changed to $U_{s_2}/U_0 = 0.04$ and to $U_{s_1}/U_0 = 0$. The power requirement now is

$$\frac{W_w}{\frac{1}{2} m_s U_0^2} = 0.0016 \quad (15)$$

which is smaller by a factor of 50! This means that propulsion is practically free when the boundary-layer-control power has been supplied and paid for (i.e., $U_{s_1} = 0$).

This observation is similar in nature to that of Wislicenus[26] concerning boundary-layer intake for open or shrouded stern propulsors. In the latter case the natural boundary layer (only partially energized to flight conditions) is exploited for propulsion, while in the former the boundary-layer-control discharge, fully energized, is presented to the propulsor.

It is seen in Table 4 that the boundary-layer-control suction-power is much larger than the propulsion power for the data of Ref. 4 ($g/L = 0.008$). It represents by far the major portion of the total power requirements.

Therefore, there is available a comparatively large mass flow m_s within the vehicle with zero relative velocity, which is begging to be used for propulsion and to be discharged with a finite U_{s_2} from the stern. It would not be very practical to discharge m_s from the vehicle at $U_{s_2} = 0$ in any event! The reader is referred to Edwards[27] for an excellent discussion on the fundamental aspects of propulsion for boundary-layer-control vehicles, which needs no repetition here.

The pumping system comprises the annular suction slot and a short annular duct leading into an axial pump stage. The discharge of this stage is assumed to be just sufficient to bring the fluid to freestream conditions, since any output

Table 3 Slot-width effects

g/L	C_{Ds}	C_{Dw}	C_Q	C_D	C_{Ds}/C_{Dw}
0.016	0.0160	0.0013	5.75	0.0173	12.3
0.016	0.0161	0.0014	5.78	0.0175	11.5
0.012	0.0176	0.0054	4.80	0.023	3.26
0.012	0.0153	0.0032	5.55	0.0185	4.80
0.008	0.0149	0.0019	5.35	0.0168	7.85
0.008	0.0147	0.0020	5.35	0.0167	7.35

increment above this level is to be charged to propulsion rather than to suction.

For large installations, such as submarines, the over-all pumping system efficiency may be expected to be 90%. For small installations, such as torpedoes, the system efficiency probably will not exceed 80%. The propulsion system conceptually comprises another and separate pump stage and an exit nozzle. Actually there will be only one axial impeller for both duties.

The suction mass-flow coefficient C_m and the suction-power coefficient $C_{Ps} = C_{Ds}$ are given in Table 4 from the experimental data of Ref. 4. It remains to compute the U_{s_2}/U_0 ratio and the propulsion power W_w (on the assumption that $U_{s_1}/U_0 = 0$.) The computation of C_m is of interest, given m_s from the data of Ref. 4,

$$C_m = \frac{m_s}{\rho U_0 L^2} = \frac{m_s}{\rho U_0 L/\mu} \cdot \frac{1}{\mu L} = \frac{m_s}{R_L} \frac{10^7}{18.1} \tag{16}$$

and

$$C_m/C_Q = (\theta_1/L)(\pi d_1/L)(U_1/U_0) \tag{17}$$

$$C_T = \frac{m_s U_0}{q}\left(\frac{U_{s_2}}{U_0}\right) = \frac{2m_s}{\rho L^2 U_0 (V^{2/3}/L^2)} \frac{U_{s_2}}{U_0} \tag{18}$$

$$C_T = 2\frac{L^2}{V^{2/3}}\left(\frac{U_{s_2}}{U_0}\right) \tag{19}$$

or

$$\frac{U_{s_2}}{U_0} = \frac{1}{2}\frac{C_T}{C_m}\left(\frac{V^{2/3}}{L^2}\right) = \frac{1C_{Dw}}{2C_m}\left(\frac{V^{2/3}}{L^2}\right) \tag{20}$$

and

$$W_w = \frac{1}{2} m_s (U_{s_2}{}^2) = \frac{1}{2} m_s U_0{}^2 \left(\frac{U_{s_2}}{U_0}\right)^2 \tag{21}$$

$$C_{Pw} = \frac{1}{2}\frac{m_s U_0{}^2}{q U_0}\left(\frac{U_{s_2}{}^2}{U_0{}^2}\right) = \frac{m_s}{\rho U_0 L^2}\left(\frac{L^2}{V^{2/3}}\right)\left(\frac{U_{s_2}}{U_0}\right)^2 \tag{22}$$

$$C_{Pw} = C_m\left(\frac{L^2}{V^{2/3}}\right)\left(\frac{U_{s_2}}{U_0}\right)^2 = \frac{1}{4} C_m \left(\frac{L^2}{V^{2/3}}\right)\left(\frac{C_T{}^2}{C_m{}^2}\right)\left(\frac{V^{2/3}}{L^2}\right)^2 \tag{23}$$

$$C_{Pw} = \frac{1}{4}\left(\frac{C_T{}^2}{C_m}\right)\left(\frac{V^{2/3}}{L^2}\right) = \frac{1}{4}\left(\frac{C_{Dw}{}^2}{C_m}\right)\left(\frac{V^{2/3}}{L^2}\right) \tag{24}$$

In other words, the propulsion power coefficient C_{Pw} is directly proportional to the square of the thrust coefficient and inversely proportional to the total suction mass-flow coefficient. The suction-power coefficient C_{Ps}, the propulsion power coefficient C_{Pw}, the total power coefficient C_P, and the mechanical power coefficient $C_P{}^*$ (assuming $\eta_P = 90\%$) are shown in Table 5 with R_L, for the case of $g/L = 0.008$. Using a set of experimental values at the highest R_L conditions,

$$U_1/U_0 = 1.20 \qquad C_T = C_{Dw} = 0.002$$
$$L^2/V^{2/3} = 6.95$$
$$C_{Ps} = 0.0142 \qquad \pi d_1/L = 0.615$$
$$C_m = 0.00386$$

Then

$$C_{Pw} = \frac{4 \times 10^{-6}}{3.86 \times 10^{-6} \times 4 \times 6.95} = 3.71 \times 10^{-5} \tag{25}$$

and

$$U_{s_2}/U_0 = \tfrac{1}{2}[0.002/(0.00386 \times 6.95)] = 0.0372 \tag{26}$$

It is to be noted that the propulsion jet needs to be only 3.7% of the flight velocity. The total power coefficient will be

$$C_P = C_{Ps} + C_{Pw} = 0.0142 + 0.0000371$$
$$C_P = 0.014238 \tag{27}$$

Assuming a pump efficiency $\eta_P = 90\%$ (for a large installation), the total mechanical power coefficient will be $C_P{}^* = C_P/\eta_P = 0.01585$.

There is a tradeoff possible between suction power and propulsion power. Figure 11 indicates ($N = 5$ curve) that it is theoretically possible (although not achieved in Ref. 4) to reduct C_Q from 4.0 to 2.5, thereby doubling θ_2 from $\theta_2/\theta_1 = 1.0$ to $\theta_2/\theta_1 = 2.0$.

Thus $C_{Ds} = 0.00885$ (assuming constant C_H); $C_{Dw} = 0.004$. Now

$$U_{s_2}/U_0 = 81.5(C_{Dw}/C_Q) = 0.072(C_{Dw}/C_m) = 0.13 \tag{28}$$

and $C_{Pw} = 0.0003$. The total mechanical power coefficient will be

$$C_P{}^* = \frac{0.00885 + 0.0003}{0.90} = \frac{0.00915}{0.90} = 0.0102$$

This tradeoff has reduced the total mechanical power by 35%. It appears then the suction power for boundary-layer control should be reduced and the wake drag allowed

Table 4 Experimental drag coefficients

R_L	C_m	C_{Ds}	C_{Dw}	C_D
4.51×10^6	4.55×10^{-3}	0.0179	0.0028	0.0207
4.41	6.32	0.0197	0.0018	0.0215
4.51	6.35	0.0193	0.0009	0.0202
4.60	9.45	0.0191	0.0003	0.0194
7.15	4.17	0.0158	0.0030	0.0188
7.20	5.18	0.0166	0.0014	0.0180
7.10	5.50	0.0167	0.0010	0.0177
7.10	6.00	0.0177	0.0009	0.0186
10.15	4.03	0.0149	0.0019	0.0168
10.0	4.12	0.0147	0.0020	0.0167
4.36	10.1	0.0207	0.0005	0.0212
6.95	4.20	0.0157	0.0024	0.0181
7.10	5.40	0.0171	0.0013	0.0184
7.05	6.23	0.0180	0.0008	0.0188
6.95	6.43	0.0177	0.0009	0.0186
9.8	3.98	0.0146	0.0027	0.0173
10.2	4.14	0.0147	0.0026	0.0173
10.1	4.23	0.0152	0.0026	0.0178
11.3	3.86	0.0142	0.0020	0.0162

Table 5 Power coefficients

R_L	C_{Ps}	C_{Pw}	C_P	$C_P{}^* = C_P/\eta_P$
4.5×10^6	0.0179	0.0000625	0.017962	0.01995
4.41	0.0197	0.0000185	0.019718	0.0219
4.51	0.0193	0.000046	0.019304	0.0214
4.6	0.0191	0.000003	0.019100	0.0212
7.15	0.0158	0.0000775	0.015877	0.0176
7.20	0.0166	0.0000136	0.016613	0.0184
7.10	0.0167	0.0000065	0.016706	0.01855
7.10	0.0177	0.0000048	0.017704	0.01965
10.15	0.0149	0.0000321	0.014932	0.0166
10.0	0.0147	0.0000350	0.014735	0.01635
4.36	0.0207	0.0000009	0.020700	0.02300
6.95	0.0157	0.0000491	0.015749	0.0175
2.10	0.0171	0.0000112	0.017111	0.0190
7.05	0.0180	0.0000037	0.018003	0.0200
6.95	0.0177	0.0000045	0.017704	0.0197
9.8	0.0146	0.0000655	0.014665	0.0163
10.2	0.0147	0.0000587	0.014758	0.0164
10.1	0.0152	0.0000578	0.015257	0.0169
11.3	0.0142	0.0000388	0.014238	0.01585

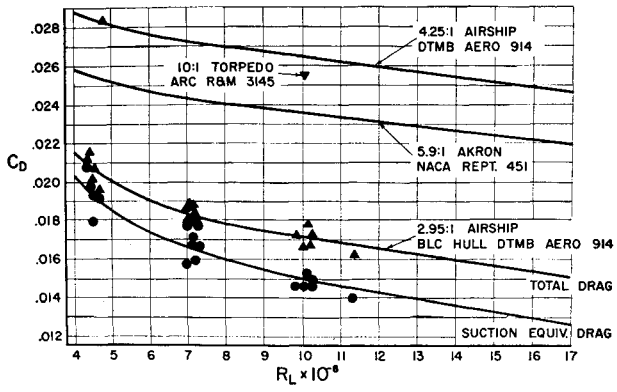

Fig. 13 Comparative drag of bare hulls without propulsion.

to increase to an approximate ratio $C_{Ds}/C_{Dw} = 2$. To achieve this, however, it will be necessary to change somewhat the hull design in the vicinity of the discontinuity, to improve the suction-slot effectiveness. This should certainly be one of the major objectives of future development.

6. Comparison with Conventional Bodies

The most conventional self-propelled submerged bodies today are high-fineness-ratio hulls (more or less streamlined) with stern propulsion by an open wake propeller. Wake propellers have been shown to have substantially improved propulsive efficiencies as compared to freestream propellers, as demonstrated experimentally by McLemore[2] and theoretically by Wislicenus[26] and others. However, it has been found that stern propellers cause a drag increment on the hull, of the nature of a pressure drag. This increment ranges from 7 to 20%, depending on the body and propeller design, and it detracts, therefore, directly from the propulsive efficiency of the hull-propellor combination.

A comparison between the integrated hull/boundary-layer-control/propulsion design (*H-BLC-P*) and conventional stern-propelled vehicles can be made in several ways, depending on the viewpoint. A traditional comparison may be made between drag coefficients of bare conventional bodies and equivalent drag coefficients (suction plus wake) of boundary-layer-control bodies. Propulsion is not considered in either case. Such a comparison is shown in Fig. 13 between the new *H-BLC-P* design and the Akron model, a blimp model, and a torpedo model. The drag gain here is impressive, 32% at $R_L = 1.7 \times 10^7$ on the basis of the Akron, 38.5% at $R_L = 1.7 \times 10^7$ on the basis of the blimp.

However, the comparison here is not too meaningful because nothing has been said about propulsion. It is suggested here that comparison be made only on the basis of the self-propelled vehicle test, where the mechanical power input to the propulsor can be measured or at least estimated.

For instance, for a 5:1 streamlined body and stern propulsion, McLemore[2] reports a $C_P^* = 0.020$ at $R_L = 1.75 \times 10^7$. This results from a $C_D = 0.021$ and an apparent propulsive efficiency of 105%, on the basis of enclosed volume. The incremental drag has been found to be 19%. The nature of this drag is demonstrated by the pressure distribution on the hull. Correcting the results to $R_L = 1.1 \times 10^7$ it is obtained $C_P^* = 0.0225/1.05 = 0.0215$. For the new *H-BLC-P* design, at the same R_L it is found $C_P^* = 0.01585$ thereby showing a mechanical power gain of 26% on the basis of the conventional vehicle.

McLemore[2] finds propulsive efficiencies up to 120% at reduced thrust and suggests that improved propellers may be designed to reach such efficiency at full thrust. In this case the power coefficient is obtained: $C_P^* = 0.0225/1.20 = 0.0188$. By the same token, it was shown previously how, with improved hull and suction-slot design, the power coefficient of the new *H-BLC-P* design may be decreased to $C_P^* = 0.0102$. Comparing now both second-generation vehicles, a power gain of 45% is made, on the basis of the conventional body. In other words, the second-generation situation will favor still more the new *H-BLC-P* design. The preceding discussion pertains only the zero angle of attack. For the new design, it is claimed that conditions will remain essentially unchanged up to a specified angle (for instance, 7°) and the only penalty would be a peripheral flow asymmetry to the pump inlet, perhaps affecting the pump efficiency. It is quite unfortunate that the wind-tunnel tests of Ref. 4 did not extend to α other than zero, and that inferences must be made on the basis of two-dimensional tests only. On the other hand, conventional stern-propelled vehicles are quite sensitive to angles of attack, as shown by McLemore.[2] For $\alpha = 7°$ the propeller thrust coefficient decreases 12% while the drag increases 40%.

Another comparison may be made on the basis of hydrodynamic noise, i.e., hull noise and wake noise. The hull noise is given by the turbulent boundary-layer pressure fluctuations, which are a strong function of the boundary-layer profile parameter $H = \delta^*/\theta$ as presented in Fig. 14. For the conventional hull the pressure fluctuations will reach 7% to 10% of freestream dynamic pressure, while for the new design H will always remain between 1.4 and 1.5, thereby assuring pressure fluctuations only of the order of 1%. The wake noise is proportional to the external drag and, therefore, to the thrust generated. For conventional vehicles the entire mechanical power is used to create thrust by open propellers in the noisiest possible manner. In the new design the total power is reduced (as much as 50%), the external thrust is quite small (less than 10% of the conventional thrust), and a shrouded propeller is used. Thus, the over-all noise situation will be much improved by the new *H-BLC-P* design.

7. Conclusions

A case has been made for the integration of hull design, boundary-layer control, and propulsion of self-propelled submerged bodies on the basis of partial wind-tunnel tests. It appears that large power gains (of the order of 50%) can be made as compared to the best streamlined body with stern wake propellers and that the power gains are much larger at angles of attack within a specified range and also at higher Reynolds numbers.

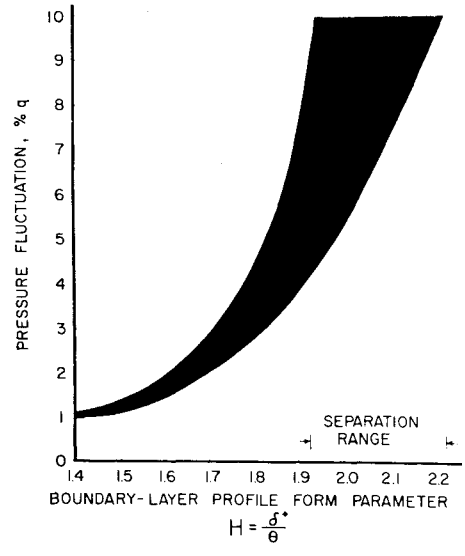

Fig. 14 Turbulent boundary-layer pressure fluctuations.

Complete large-scale wind-tunnel tests of a self-propelled model (such as carried out by McLemore[2] for the conventional streamlined body with stern wake propellers) are needed to provide satisfactory experimental evidence for this design integration concept. A development program should be planned for three fineness ratios, 1.5:1, 2:1, and 3:1 and for discontinuity locations as far back as 90%. Particular attention should be paid to the suction-slot design and the hull contour in the vicinity of the discontinuity, so as to minimize the minimum value of C_Q sufficient to stabilize the boundary-layer crossing the pressure rise. Following the aerodynamic development, preliminary design studies should be made for several typical submarine applications in order to explore the new design freedom allowed by the present concept of hull/boundary-layer-control/propulsion integration.

References

[1] Goldschmied, F. R., "Proposal for the study of application of boundary-layer control to lighter-than-air craft," Goodyear Aircraft Rept. GER-5796 (1954).

[2] McLemore, H. C., "Wind-tunnel tests of a $\frac{1}{20}$ scale airship model with stern propellers," NASA TN D-1026 (January 1962).

[3] Goldschmied, F. R., "A theoretical aerodynamic analysis of a boundary-layer controlled airship hull," Goodyear Aircraft Rept. GER-6251 (September 1954).

[4] Cerreta, P. A., "Wind-tunnel investigation of the drag of a proposed boundary-layer-controlled airship," David Taylor Model Basin Aero Rept. 914 (March 1957).

[5] "An investigation of a boundary-layer-controlled airship," Goodyear Aircraft Rept. GER-8399 (October 1957).

[6] McCormick, B. W., Eisenhuth, J. J., and Lynn, J. E., "A study of torpedo propellers—Part I," Pennsylvania State Univ., Ordnance Research Lab. Rept. NORD 16597-5 (March 30, 1956).

[7] Gearhart, W. S. and Henderson, R. E., "Selection of a propulsor for a submersible system," J. Aircraft **3**, 84–90 (1966).

[8] Goldschmied, F. R., "An approach to turbulent incompressible separation under adverse pressure gradients," J. Aircraft **2**, 108–115 (1965).

[9] Lighthill, M. J., "A new method of two-dimensional aerodynamic design," British Aeronautical Research Council R&M 2112 (April 1945).

[10] Richards, E. J. and Burge, C. H., "An airfoil designed to give laminar flow over the whole surface with boundary-layer suction," British Aeronautical Research Council R&M 2263 (June 1943).

[11] Head, M. R., "Aerofoils with suction applied at the pressure minimum," *Boundary Layer and Flow Control*, edited by G. V. Lachmann (Pergamon Press Inc., New York, 1961), Vol. I, pp. 106–108.

[12] Thwaites, B., "Slot suction," p. 232; also "Slot suction on aerofoils specially designed for very low drag," pp. 243–249, *Incompressible Aerodynamics* (Clarendon Press, Oxford, England, 1960).

[13] Schlichting, H., *Boundary-Layer Theory* (McGraw-Hill Book Company Inc., New York, 1960), 4th ed.

[14] Gregory, N. and Walker, W. S., "Further wind-tunnel tests on a 30% symmetrical suction aerofoil with a movable flap," British Aeronautical Research Council R&M 2287 (July 1946).

[15] Goldschmied, F. R., "Incompressible potential flow velocity distribution over bodies of revolution," Goodyear Aircraft Rept. GER-5235 (1953).

[16] Thwaites, B., "Uniform flow past bodies of revolution," *Incompressible Aerodynamics* (Clarendon Press, Oxford, England, 1960), Chap. IX, pp. 369–418.

[17] Cheers, F. and Rayner, W. G., "Tests in the N. P. L. electric tank on a 4:1 axisymmetrical diffuser having a discontinuity in the wall velocity," British Aeronautical Research Council Current Paper 2 (March 1946).

[18] Goldschmied, F. R., "Calibration of the three-dimensional electric analog tank," Westinghouse Electric Corp., ADR-1 (December 1954).

[19] Freeman, H. B., "Pressure distribution measurements on the hull and fins of a $\frac{1}{40}$ scale model of the airship Akron," NACA Rept. 443 (1932).

[20] Allen, H. J., "Pressure distribution and some effects of viscosity on slender inclined bodies of revolution," NACA TN 2044 (March 1950).

[21] Rodgers, E. J., "Real flow over a body of revolution at angle of attack," Pennsylvania State Univ., Ordnance Research Lab. TM 5 2420–13 (March 1963).

[22] Boltz, F. W., "Boundary-layer transition characteristics on two bodies of revolution, a flat plate and an unswept wing in a low-turbulence wind-tunnel," NASA TN D-309 (March 1960).

[23] Truckenbrodt, E., "A method of quadrature for calculation of the laminar and turbulent boundary-layer in case of plane and rotationally symmetrical flow," NACA TM 1379 (May 1955).

[24] Gregory, N., "Note on G. I. Taylor's criterion for the rate of boundary-layer suction at a velocity discontinuity," British Aeronautical Research Council R&M 2496 (May 1947).

[25] Preston, J. H., Gregory, N., and Rawcliffe, A. G., "The theoretical estimation of power requirements for slot-suction aerofoils, with numerical results for two thick Griffith sections," British Aeronautical Research Council R&M 2577 (June 1948).

[26] Wislicenus, G. F., "Hydrodynamics and propulsion of submerged bodies," ARS J. **30**, 1140–1148 (1960).

[27] Edwards, J. B., "Fundamental aspects of propulsion for laminar flow aircraft," *Boundary Layer and Flow Control*, edited by G. V. Lachmann (Pergamon Press Inc., New York, 1961), Vol. II, pp. 1077–1100.